METAL CUTTING & TOOL DESIGN

Unit-2

L 15.1 Theory of Ernst & Merchant

This story is suggested in 1941 based on “principle of minimum energy consumption”.

1. Cutting velocity always remains constant.
2. Cutting edge of the tool remains sharp throughout cutting and there is no contact between the workpiece and tool flank.
3. There is no sideways flow of chip.
4. Only continuous chip is produced.
5. There is no built-up Edge.
6. No consideration is made of the inertia force of the chip.
7. The behaviour of chip is like that of a free body which is in the state of a stable equilibrium due to the action of two resultant forces which are equal opposite and collinear.

The basis of Ernst and Merchant theory was this suggestion that the shear angle would take up such a value as to reduce the work one in cutting a minimum. For this, is necessary to develop an expression

for cutting force in terms of shear angle and then obtain the value of shear angle for which cutting force

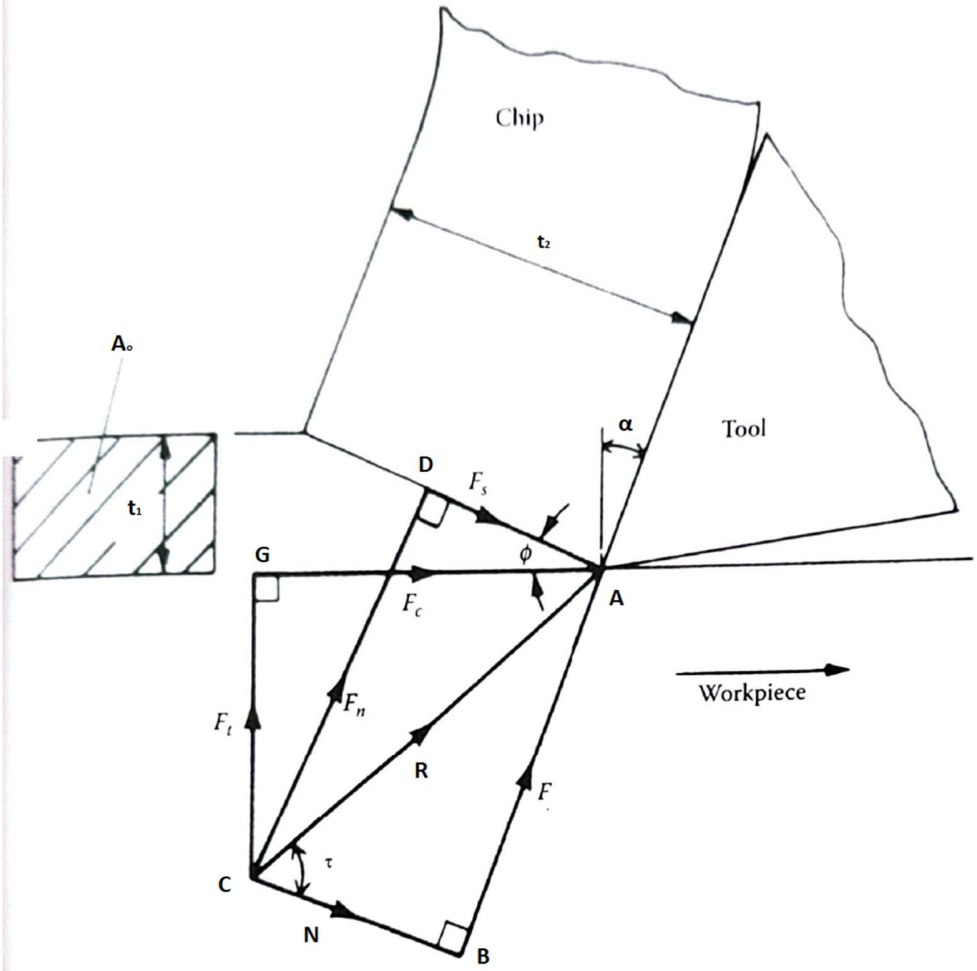

FIGURE 15.1 Force diagram for orthogonal cutting, where R = resultant tool force, F_c = cutting force, F_t = thrust force, F_s = shear force on shear plane, F = frictional force on tool face, N = normal force on tool face, ϕ = shear angle, α = working normal rake, τ = mean friction angle on tool face, t_1 = undeformed chip thickness, and t_2 = chip thickness.

is a minimum.

From Fig. 15.1

$$F_s = R \cos(\phi - \tau - \alpha) \quad \text{.....(1)}$$

$$F_s = \tau_s A_s = \frac{\tau_s A_o}{\sin \phi} \quad \text{.....(2)}$$

where

τ_s = shear strength of the work material on the shear plane

As = area of the shear plane

A_o = cross -sectional area of the uncut chip

τ = mean angle of friction between chip and tool (given by merchant F/ N)

α = working normal rake

From Equation (1) and Equation (2):

$$R = \frac{\tau s Ao}{sin\emptyset} \cdot \frac{1}{\cos(\emptyset - \tau - \alpha)} \quad \text{.....(3)}$$

Now by geometry:

$$F_c = R \cos(\tau - \alpha) \quad \text{.....(4)}$$

Hence from Equation (3) and Equation (4):

$$F_c = \frac{\tau s \; Ao \; Cos \; (\tau - \alpha)}{sin\emptyset \cos(\emptyset + \tau - \alpha)} \quad \text{.....(5)}$$

Equation (5) may now be differentiated with respect to Shear Angle ϕ and equated to zero to find the value of Shear Angle ϕ for which Fc is a minimum. The required value is given by

$$2\emptyset + \tau - \alpha = \frac{\pi}{2} \quad \text{.....(6)}$$

L 15.2 Merchant Modification

Merchant found that this theory agreed well with experimental results obtained when cutting synthetic plastics but agreed poorly with experimental results obtained for steel machined with a sintered carbide tool.

It should be noted that in differentiating Equation (5) with respect to ϕ, it was assumed that Ao, α and τ_s would be independent of ϕ. On reconsidering these assumptions, Merchant decided to include in a modified analysis the relationship

$$\tau_s = \tau_{so} + k\sigma_s \quad \text{----------(7)}$$

which indicates that the shear strength of the material τ_s increases linearly with increase in normal stress σ_s, as on the shear plane (Figure 15.2); at zero normal stress τ_s is equal to τ_{so}. This assumption agreed

with the work of 'Bridgman', where, in experiments on polycrystalline metals, the shear strength was shown to be dependent on the normal stress on the plane of shear.

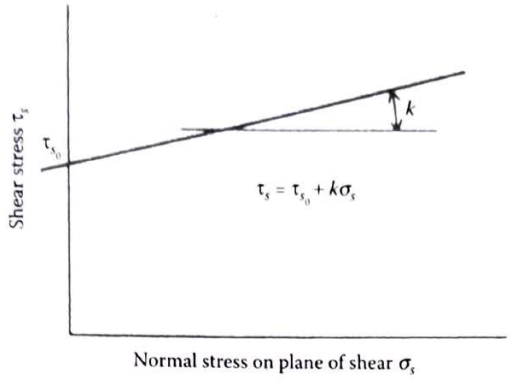

Fig.15.2 Dependence of τ_s and σ_s assumed in Merchant's second theory.

Now from Figure 15.2

$$F_n = R \sin(\phi + \tau - \alpha) \quad \text{.....(8)}$$

and

$$F_n = \sigma_s A_s = \sigma_s A_o / \sin\phi \quad \text{.....(9)}$$

From eq. (8) & (9)

$$\sigma_s = \frac{\sin\emptyset}{Ao} R \sin(\emptyset + \tau - \alpha) \quad \text{.....(10)}$$

Combining eq. (3) & (10)

$$\sigma s = \frac{\sin\emptyset}{Ao} . \frac{\tau s Ao}{sin\emptyset} . \frac{\sin(\emptyset + \tau - \alpha)}{\cos(\emptyset + \tau - \alpha)}$$

$$\sigma_s = \tau_s \tan(\emptyset + \tau - \alpha)$$

$$\tau_s = \sigma_s \cot(\emptyset + \tau - \alpha) \quad \text{.....(11)}$$

from eq. (7) & (11)

$$\tau_s = \tau_{so} + k\frac{\tau s}{\cot(\emptyset+\tau-\alpha)}$$

$$\tau s \left[1 - \frac{k}{\cot(\emptyset+\tau-\alpha)}\right] = \tau_{so}$$

$$\tau_s = \frac{\tau so}{1-\frac{k}{\cot(\emptyset+\tau-\alpha)}}$$

$$\tau_s = \frac{\tau so}{1-k\ \tan(\emptyset+\tau-\alpha)} \quad \text{.....(12)}$$

This equation shows how the value of τ_s may be affected by changes in ϕ, and is now inserted in Equation (5) to give a new equation for Fc, in terms of ϕ,:

$$Fc = \frac{\tau so\ Ao \cos(\tau-\alpha)}{sin\emptyset\ \cos(\emptyset+\tau-\alpha)\ [1-k\ \tan(\emptyset+\tau-\alpha)]} \quad \text{.....(13)}$$

It is now assumed that k and τ_{so} are constants for the work material and that Ao and α are constants for the cutting operation. Thus Equation (13) may be differentiated to give the new value of ϕ. The resulting expression is

$$\boxed{2\phi + \tau - \alpha = C} \quad \text{.....(14)}$$

[C= constant, it's depends on the slope of line, k]

L 16.1 Theory of Lee & Shaffer

The theory of Lee & shaffer was the result of an attempt to apply simplified plasticity analysis to the problem of orthogonal metal cutting. Certain assumptions regarding the behavior of the work material under stress were made as follows:

1. The material is rigid plastic, which means that we elastic strain is negligible during deformation and that once the yield point is exceeded deformation take place at constant stress.
2. The behavior of the material is independent of the rate of deformation.
3. The effect of temperature increases during deformation are neglected.
4. The inertia effects resulting from acceleration of the material during deformation are neglected.
5. Tool tip is sharp.
6. Continuous chip is formed.
7. Stress are uniform on the rake face (μ is constant).

The assumptions should closely approximate the actual behavior of the material during cutting because of the very high stress and strain rate that occurs in the cutting process. It is know that the rate of work hardening of most metals decreases rapidly with increasing strain and that the

effect of a high strain rate is to raise the yield strength of a metal with respect to its ultimate stress. One approach to solve problem in plasticity is to construct a slip line field.

Slip line field solution

In general, 3-D deformation problem is difficult to analyze. However, often it can be reduced to a 2-D (plane strain) problem.

Slip line field theory is an approach that has been widely used for solution of plain strain problems. It is based on the fact that any general state of stress in plane strain consist of pure shear and hydrostatic pressure. The slip lines are lines of maximum shear stress and show the direction of shear yield strength in pure shear at a given point. They come in orthogonal pairs and are designated as η and β lines.

The silent properties of slip line are as follows:

a. Shear strain is maximum along the slip lines.
b. Linear strain is zero along the tangent to the slip lines.
c. Slip lines may in general be curved, but if the stress distribution in the deformation zone is uniform then they are represented as straight lines.
d. The tangents of η and β lines, i.e. the directions of maximum shear stresses make an angle π/4 with the direction of principal stresses.
e. The line of action off the algebraically largest principal stress lies in the first and third quadrants.
f. On the free surface, there can be no normal stress therefore $\sigma_3 = 0$. Assuming be hydrostatic compressive stress on all the faces of an element of the free surface equal to "ρ".

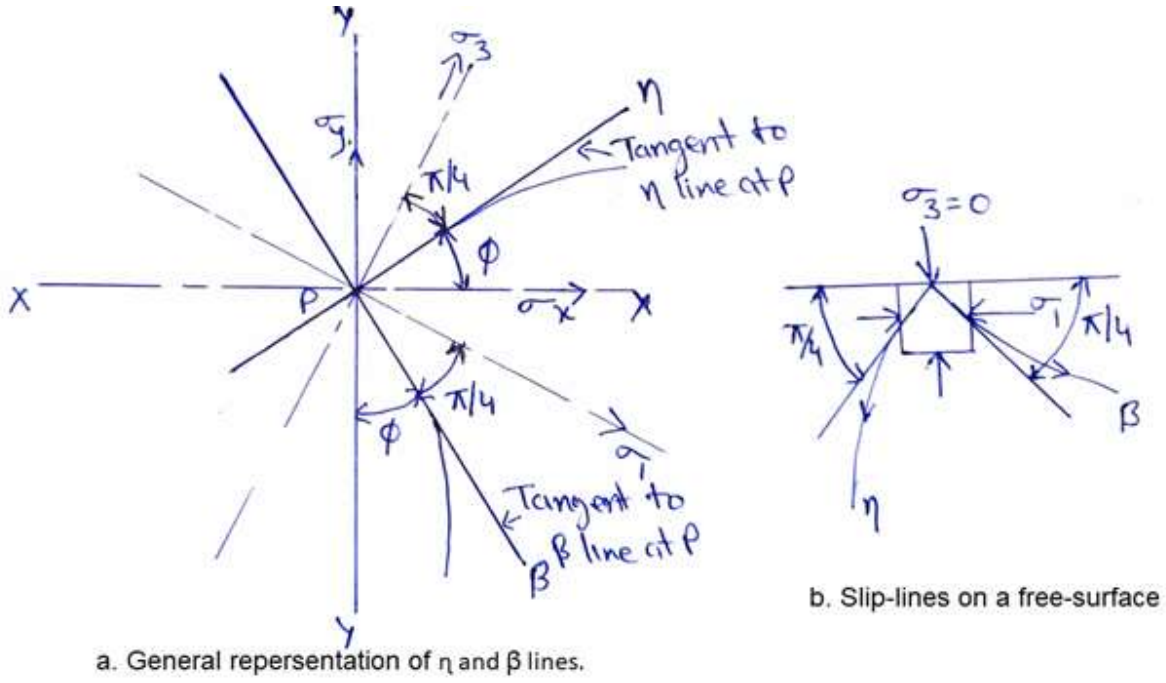

a. General repersentation of η and β lines.

b. Slip-lines on a free-surface

Fig. 16.1 Slip line field

Lee & Shaffer's Shear Angle Relation

Several shear angle relations based on slip line field approach have been developed. The earliest and the simplest of all of them proposed by Lee & Shaffer in 1951.

They assume that the material ahead of the tool is ideally plastic and that the shear plane coincides with the direction of maximum shear stress.

The further assumed that is slip field exists within the chip to transmit the cutting forces from the shear plane to the tool face.

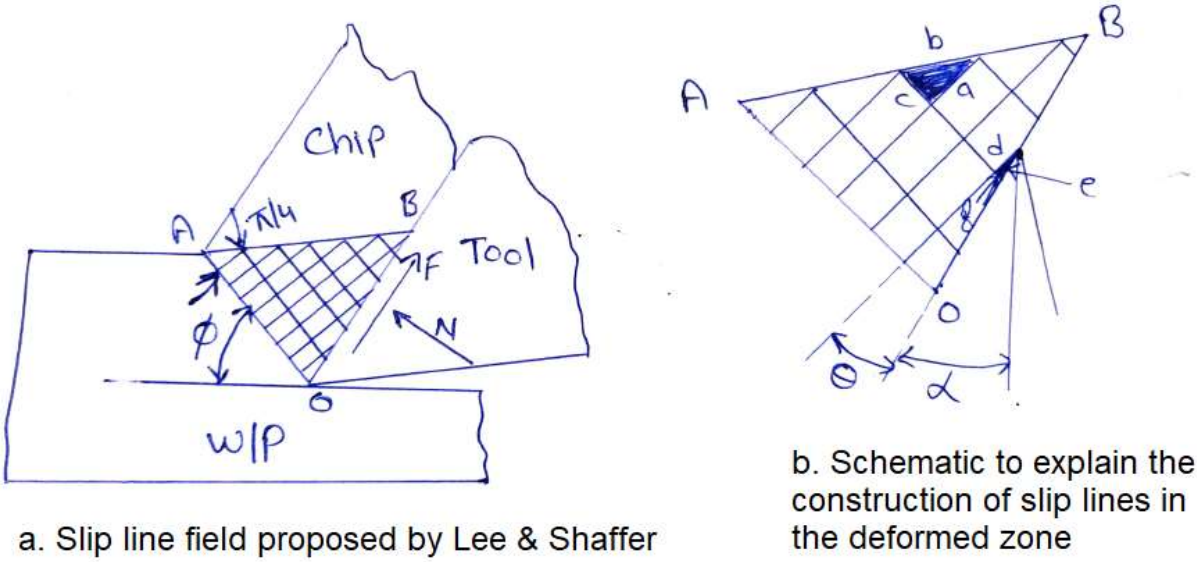

a. Slip line field proposed by Lee & Shaffer

b. Schematic to explain the construction of slip lines in the deformed zone

Fig. 16.2 Lee & Shaffer's slip line field

By the figure 16.2 chip shear in plane OA, it retains some shearing stress in a certain deformed zone OAB and only in the plane AB the sharing becomes complete, i.e. plane AB is a free surface on which the shear stress and normal stress both are equal to zero. Hence, AB is a principal plane in which the principal stress is zero.

The following point regarding these slip line field shown in figure 16.2:

i. As par property 'B' off the slip lines, two set of orthogonal slip line will emanate from different point of AB at an angle π/4. Assuming uniform stress distribution in deformed zone OAB, the slip lines are shown as straight lines.
ii. As OA is assumed to be coincident with the direction of maximum shear stress and AB is coincident with the direction of one of principle stress angle OAB = 45.
iii. In view of 'i' & 'ii' above, one set of slip lines emanating from points of AB must be incident on OA at right angle to it. Further, considering property 'e' off the slip lines, this set of slip lines must be associated with the algebraically largest principal stress. As one of the principle stress that lies among the free surface AB is zero, the other perpendicular to it will be equals 2τ.

Determination of Shear Angle by Mohr's Circle

1. Let us consider an element 'abc' in plain AB and another element 'def' on the tool face.
2. If the mohr's circle is drawn for the state of stress in the deformed on 'OAB', the center of the circle where the shear and normal stress are both zero will be represented the stress in plane 'b' of element 'abc'.

3. Plane ‘a’ of element ‘abc’ and ‘d’ of element ‘def’ are inclined to ‘b’ at π/4 in the positive direction.
4. Accordingly, their state of stress is represented by point (a,d) on the mohr’s circle.
5. Similarly, the state of stress of plane ‘c’ & ‘f’ that are inclined to ‘b’ at π/4 in the negative direction.

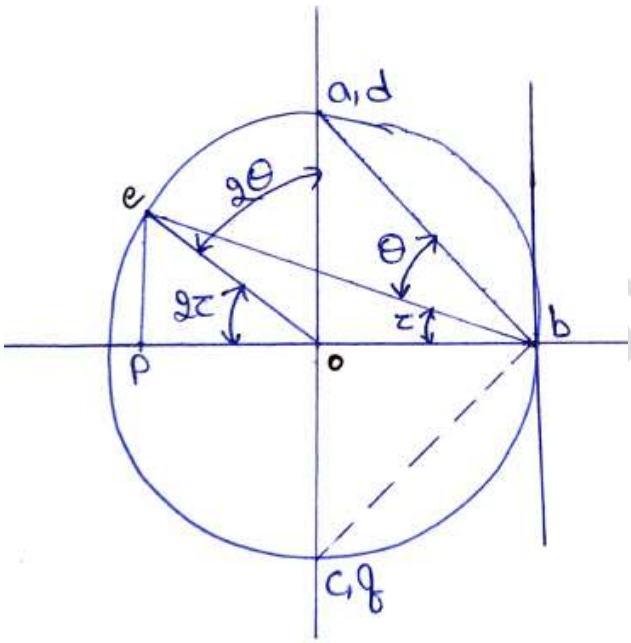

Fig. 16.3 Mohr’s circle representing the state of stress in the deformed zone

6. The stress is at the tool face are given by plane ‘e’ of element ‘def’. Since plane ‘e’ makes angle θ with plane ‘d’, the location of point ‘e’ on the mohr’s circle is obtained by drawing a line making angle 2θ with line [o, (a, d)].
7. Applying the theorem that the angle subtended by a chord at the center of a circle is twice the angle subtended by it at periphery. We observe that:

   Angle [(a, d), o, e] = 2θ

   Angle [(a, d), b, e] = θ
8. The coordinate of point ‘e’ gives shear angle stress (frictional) and abscissa the normal stress on the tool face.
9. Hence, the friction angle ‘τ’ is found from the following relation:

$$\mu = \tan\tau = \frac{Pe}{Pb} = \frac{\tau s}{\sigma s}$$

10. From the Mohr’s circle

$$\theta = \frac{\pi}{4} - \tau$$

11. From the geometrical construction of the deformed zone

$$\emptyset = \theta + \alpha$$

12. substituting the value of θ in above equation

$$\text{ø} = \frac{\pi}{4} - \tau + \alpha$$

or

$$\text{ø} = \frac{\pi}{4} - (\tau - \alpha)$$

L 17.1 Friction in Metal Cutting

It is clear from the preceding discussion that, by some mechanism not completely understood, the frictional behavior on the tool face affects the geometry of the cutting process. Before the frictional conditions in metal cutting are considered, it is necessary to discuss the nature of friction between dry sliding surfaces.

Amontons ' laws of friction, formulated in 1699, state that friction is independent of the apparent area of contact and proportional to the normal load between the two surfaces. In 1785, Coulomb verified these laws and made a further observation, that the coefficient of friction is substantially independent of the speed of sliding. The work of Bowden and Tabor has contributed much to the explanation of these empirical laws.

Microscopic examination shows that even the most carefully prepared "flat" metallic surfaces consist of numerous hills and valleys. When two surfaces are placed together, contact is established at the summits of only a few irregularities (asperities) in each surface (Figure 17.1a). If a normal load is applied, yielding occurs at the tips of the contacting asperities, and the real area of contact Ar, increases until it is capable of supporting the applied load. For the vast majority of engineering applications, this real area of contact Ar is only a small fraction of the apparent contact area Aa and is given by

$$A_r = \frac{F_n}{\sigma_y} \quad \text{.....1}$$

Where Fn is the normal force, and σy is the yield pressure of the softer metal.

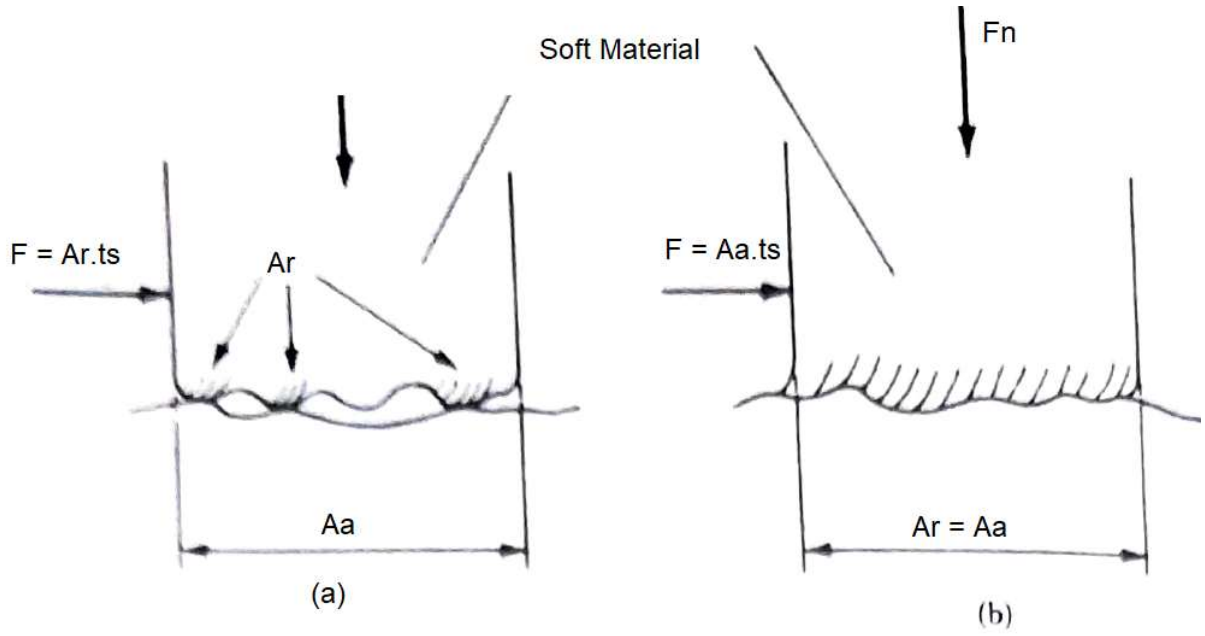

Fig. 17.1 Suggested frictional behavior for a soft material, Where F = frictional force, Fn = normal force, Ar = real area of contact, Aa = apparent are of contact and τs = Shear strength of softer metal. (a) Sliding friction; (b) Sticking friction.

The adhesion resulting from the intimate metallic contact of these asperities has been termed welding, and when sliding takes place, a force is required for continual shearing of the welded junctions at the tips of these asperities. The total frictional force F is therefore given by

$$F = \tau_s A_r \quad \text{.....2}$$

Where τs is the shear strength of the softer metal.

Thus, from Equation 1 and Equation 2 the equivalent coefficient of friction is given by

$$\mu = \frac{F}{F_n} = \frac{\tau_s}{\sigma_y} \quad \text{.....3}$$

Equation 3 shows that the coefficient of friction is independent of the apparent contact area and since the ratio τs/σy would be expected to be Substantially constant for a given metal, the frictional force is proportional to the normal load (i.e., μ is constant). These results are consistent with the laws of dry sliding friction.

During metal cutting. It has generally been observed that the mean coefficient of friction between the 'chip and tool can vary considerably and is affected by changes in cutting speed, rake angle, and so on. This variance of the mean coefficient of friction results from the very high normal pressures that exist at the chip-tool interface. For example, when steel is machined, these

normal pressure can be as high as 3.5 GN/m^2 and can cause the real area of contact to approach, or become equal to, the apparent contact area over a portion of the chip tool interface (i.e., Ar/Aa = equals unity). Thus, under these circumstances Ar has reached its maximum value and is constant. The frictional force F is still given by Equation 2 but is now independent of the normal force Fn, and the ordinary laws of friction no longer apply. Under these conditions the shearing action is no longer confined to surface asperities but takes place within the body of the softer metal (Figure 17.1).

Consideration of frictional behavior in metal cutting has led to the model of orthogonal cutting with a continuous chip and no built-up edge shown in Figure 17.2. Here the normal stresses between the chip and the tool are sufficiently high to cause Ar/Aa to approach unity over the region of length *l*st adjacent to the tool cutting edge, termed the sticking region. In the length $l_f - l_{st}$ extended from the end of the sticking region to the point where the chip loses contact with the tool, the ratio Ar/Aa is less than unity, and therefore the coefficient of friction is constant: this region has been termed the sliding region.

ln previous work, evidence of the sticking mode of frictional contact was produced by examination of the under surface of the chip on specimens where the cutting action had suddenly been stopped. It was observed that in a region adjacent to the tool cutting edge, the grinding marks on the tool face were imprinted on the under surface of the chip, indicating that no relative motion between the chip and the tool had occurred and that the real and apparent area of contact are equal in this region. These observations have been confirmed optically using transparent sapphire tools and high-speed photography.

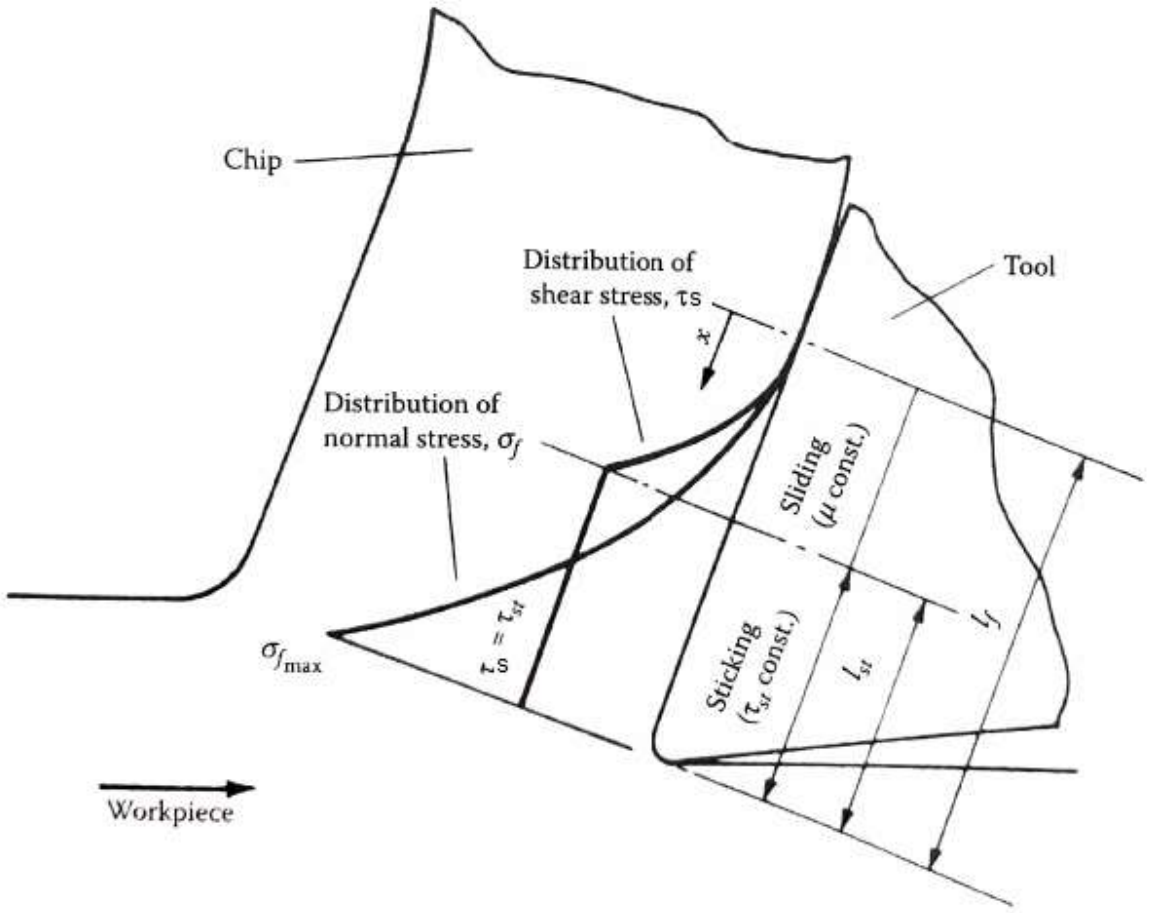

Fig. 17.2 Model of the chip-tool friction in orthogonal cutting, where σ_{fmax} = Max. normal stress, σ_f = normal stress, τ_s = shear stress, τ_{st} = Shear strength of the chip material in the sticking region, l_f =chip-tool contact length, l_{st} = length of sticking region

Under conditions of sticking friction, the mean angle of friction on the tool face will depend on the form of the normal stress distribution, the chip-tool contact length l_f, the mean shear strength of the chip material in the sticking region, and the coefficient of friction in the sliding region. Clearly, a single value of the mean angle of friction is insufficient to describe completely the frictional conditions on the tool face.

An analysis of the stress distribution on the tool face shown in Figure 17.2 has been presented by Zorev. It was shown that the mean angle of friction is mainly dependent on the mean normal stress on the tool face, and this result may be used to explain the effect of changes in working normal rake α on the mean friction angle τ. As α increases, the component of the resultant tool force normal to the tool face will decrease, and the ref ore the mean normal stress will decrease. However, the mean shear stress remains roughly constant and therefore an increase in α would

be expected to increase the mean angle of friction τ. This result is in accordance with the findings of experimental work where an increase in α has been shown to result in an increase in τ for a wide variety of work materials. The general form of the rake face stress distributions shown in Figure 17.2 have been observed experimentally from photo-elastic measurements and using split-tool dynamometers. These methods do not allow the stresses to be determined very close to cutting edge, but there is evidence to indicate that the normal stress may be constant in the sticking region close to the cutting edge.

L 18.1 Heat in Metal Cutting

A considerable amount of heat is generated in the process of metal cutting the three reasons where heat is developed in machining process:

1. **The Primary Shear Zone**

   It is the region in which actual plastic deformation of the metal occurs during machining.

   Due to this deformation, heat is generated. A portion of this heat is carried away by the Chip, due to which its temperature is raised. The rest of the heat is retained by the workpiece. It is known as Primary Deformation Zone.

2. **Tool-Chip Interface**

   As the chip slides upward s along the face of the tool friction occurs between their surfaces, due to which heat is generated. A part of this heat is carried by the Chip, which further raises the temperature of the chip, and the rest transfer red to the tool and the coolant. This area is known as Secondary Deformation Zone.

   It is reckoned that the amount of heat generated due to friction increases with the increase in cutting speed. However, it is not appreciably affected with the increase in depth of cut. When the feed rate is increased the amount of frictional heat generated is relatively low. But, in that case, the surface finish obtained is inferior.

3. **Tool-workpiece Interface**

   That portion of the tool flank which rubs against the work surface is another source of heat generation due to friction. This heat is also shared by the tool, workpiece and the coolant used. It is more pronounced when the tool is not sufficiently sharp.

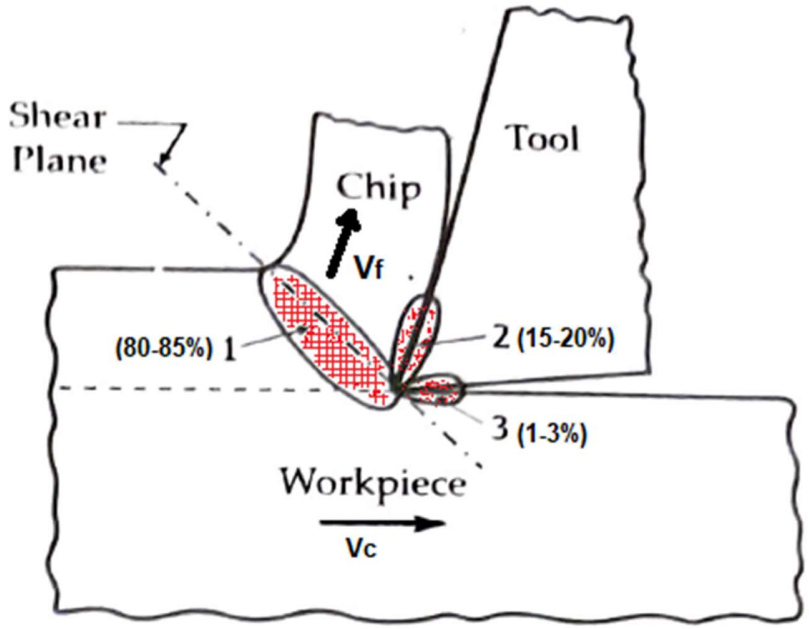

Fig. 18.1 Regions of Heat in Metal Cutting

- 80 to 85% of heat is generated in the shear zone
- 15 to 20% of heat is generated in the chip tool interface
- 1 to 3% heat is generated in tool workpiece interface zone
- 80% of heat generated is carried away by the chip
- 15 to 20% heat flow into the tool
- 5% heat flow into the workpiece

The temperature at the chip deformation zone will be high enough to influence the tool were and friction during the cutting process. As the temperature increases the hardness of the two decreases and it became more plastic thereby the tool fails by plastic deformation, becomes blunt and lose its geometry.

L 18.2 HEAT GENERATION IN METAL CUTTING

It has been stated earlier that the rate of energy consumption during machining Pm is given by

$$P_m = F_c \, . \, V_c \; .....(1)$$

where Fc is the cutting component of the resultant tool force, and Vc is the cutting speed.

When a material is deformed elastically, the energy required for the operation is stored in the material as strain energy, and no heat is generated. However, when a material is deformed plastically, most of the energy used is converted into heat. In metal cutting the material is

subjected to extremely high strains, and the elastic deformation forms a very small proportion of the total deformation; therefore, it may be assumed that all the energy is converted into heat.

Conversion of energy into heat occurs in the two principal regions of plastic deformation the shear zone, or primary deformation zone and the secondary deformation zone or Tool-Chip Interface. If, as in most practical circumstances, the cutting tool is not perfectly sharp, a third heat source Tool-workpiece Interface would be present due to friction between the tool and the new workpiece surface. However, unless the tool is severely worn, this heat source would be small and is neglected in the present analysis. Thus,

$$P_m = P_s + P_f \quad \text{.....(2)}$$

Where,

Ps = Heat generation at the primary shear zone

P_f = Heat generation at the secondary deformation zone

$$P_f = F\, V_f \quad \text{.....(3)}$$

Where,

F = Frictional force on the tool face

V_f = Chip flow velocity

L 19.1 TEMPERATURE DISTRIBUTION IN METAL CUTTING

Figure 18.2 shows an experimentally determined temperature distribution in the workpiece and the chip during orthogonal metal cutting [2. This is a typical temperature distribution for orthogonal chip formation. As a point X in the material, which is moving toward the cutting tool, approaches and passes through the primary deformation zone, it is heated until it leaves the zone and is carried away within the chip. Point Y, however, passes through both deformation zones, and it is heated until it has left the region of secondary deformation. It is then cooled as the heat is conducted into the body of the chip, and eventually the chip achieves a uniform temperature throughout. Thus, the maximum temperature occurs along the tool face some distance from the cutting edge. Point Z, which remains in the workpiece, is heated by the conduction of heat from the primary deformation zone. Some heat is conducted from the secondary deformation zone into the body of the tool. Thus,

$$P_m = \phi_c + \phi_w + \phi_t \quad \text{.....(4)}$$

where

P_m = total rate of heat generation

ϕ_c = rate of heat transportation by the chip

ϕ_w = rate of heat conduction into the workpiece

ϕ_t = rate of heat conduction into the tool

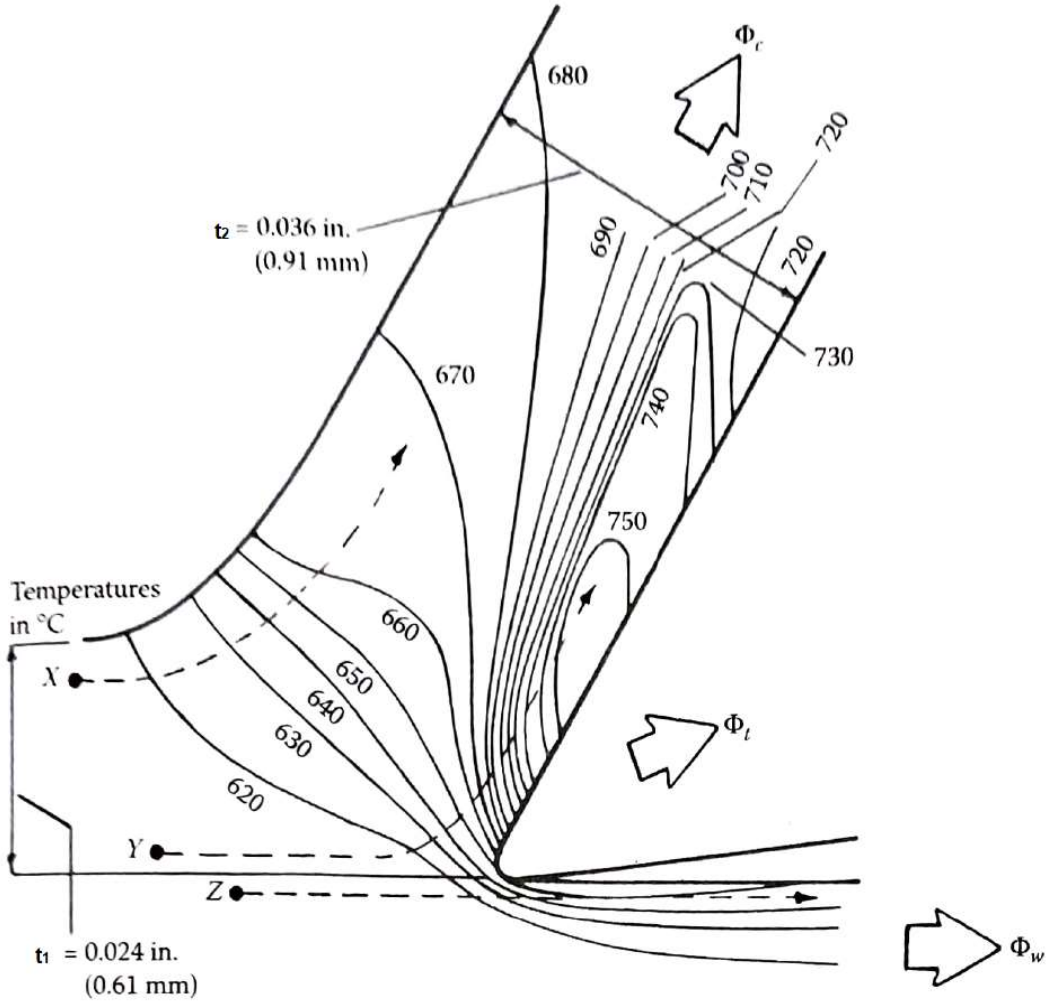

FIGURE 18.2 Temperature distribution in workpiece and chip during orthogonal cutting (obtained from an infrared photograph) for free-cutting mild steel where the cutting speed is 75 ft/min (0.38 m/s), the width of cut is 0.25 in. (6.35 mm), the working normal rake is 30 degrees, and the workpiece temperature is 611 °C. (Boothroyd, G., Proc. Inst. Mech. Eng., Vol. 177, 789, 1963.)

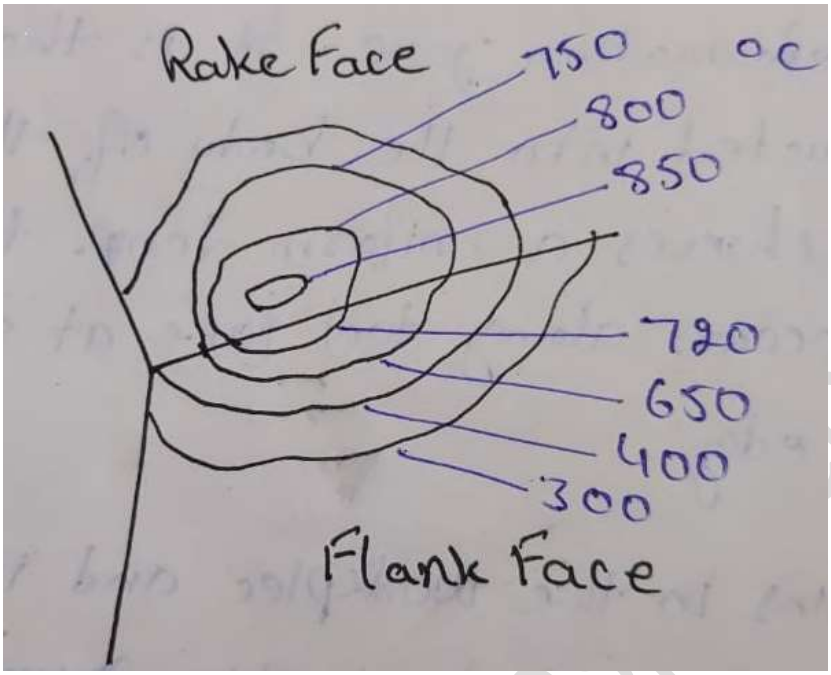

Fig. 18.3 Temp. distribution on the tool

L 20.1 TEMPERATURE IN THE DEFORMATION ZONE

Average Temperature in the Primary Deformation Zone

When a material particle moves across the primary deformation zone, the temp. rise is given by (Boothroyd-1963)

$$\theta p = \frac{(1-h)Ps}{\rho\ C\ Vc\ t1\ b} \qquad \text{.....(1)}$$

Where,

θp = Temp. rise in Primary deformation zone

h = Fraction of primary heat which goes to the workpiece

ρ = Density of the material

C = Specific heat of the material

t_1 = Uncut chip thickness

b = Width of the cut

Vc = Cutting speed

$$h = 0.5 \ln\left(\frac{27.5}{H \tan\phi}\right) \quad \text{.....(2)}$$

Where,

h is the function of shear angle and its non-dimensional quantity

H = Thermal number

$$H = \frac{\rho\, C\, Vc\, t1}{K} \quad \text{.....(3)}$$

Where,

K = Thermal conductivity of the material

Average Temperature in the Secondary Deformation Zone

The maximum temperature in the chip occur s where the material leaves the secondary deformation zone and is given by

$$\theta_{max} = \theta_o + \theta_p + \theta_s \quad \text{.....(4)}$$

where

θ_o = initial workpiece temperature

θ_p = temperature rise of the material passing through the primary deformation zone

θ_s = temperature rise of the material passing through the secondary deformation zone

The max. temp. rise in θ_s, when the material particle passes through the secondary deformation zone along the rake face of the tool can be approximately expressed as

$$\theta s \approx 1.13 \sqrt{\frac{H.t2}{l}} \left[\frac{Pf}{\rho\, C\, Vc\, b\, t1}\right] \quad \text{.....(5)}$$

l = length of contact between tool and chip

$$\frac{l}{t2} = [1 + (\tan\phi - \alpha)] \quad \text{.....(6)}$$

For average temp.

$$\theta_s = \frac{Pf}{\rho\ C\ Vc\ b\ t1} \quad \text{.....(7)}$$

Put Eq. (6) and (3) in eq (5)

$$\theta s = 1.13\sqrt{\frac{1}{\rho\ C\ Vc\ b\ t1\ k\ [1+(tan\phi - \alpha)]}} \cdot \frac{Pf}{b} \quad \text{.....(8)}$$

also,

$$\theta ov\ \boldsymbol{\alpha}\ Uc\ \sqrt{\frac{Vc\ t1}{K\ \rho\ C}} \quad \text{.....(9)}$$

Θov = Overall temp. rise in chip tool interface

Uc = Specific energy

L 21.1 THE MEASUREMENT OF CUTTING TEMPERATURES

A number of methods have been developed for the measurements of temperatures in metal cutting. Some of these methods only make it possible for the average cutting temperatures to be determined, but effective methods are available for determining temperature distributions in the workpiece, chip, and tool near the cutting edge.

A. WORK-TOOL THERMOCOUPLE

A technique widely used to study cutting temperatures is the work-tool thermocouple technique. In this technique the electromotive force (emf) generated at the junction between the workpiece and tool is taken as a measure of the temperatures in this region. A typical work-tool thermocouple arrangement on a lathe is shown in Figure 18.4. It is important when using this technique to insulate the thermocouple circuit from the machine and to use the same circuit when calibrating the thermocouple. It may be assumed that the reading given by this method is an indication of the mean temperature along the chip-tool interface. This technique has been used extensively in the past to investigate the effects of changes in cutting conditions on cutting temperatures and to obtain empirical relationships between temperature and cutting-tool wear rate. However, the work-tool thermocouple method is limited because it gives no indication of the distribution of temperature along the tool rake face.

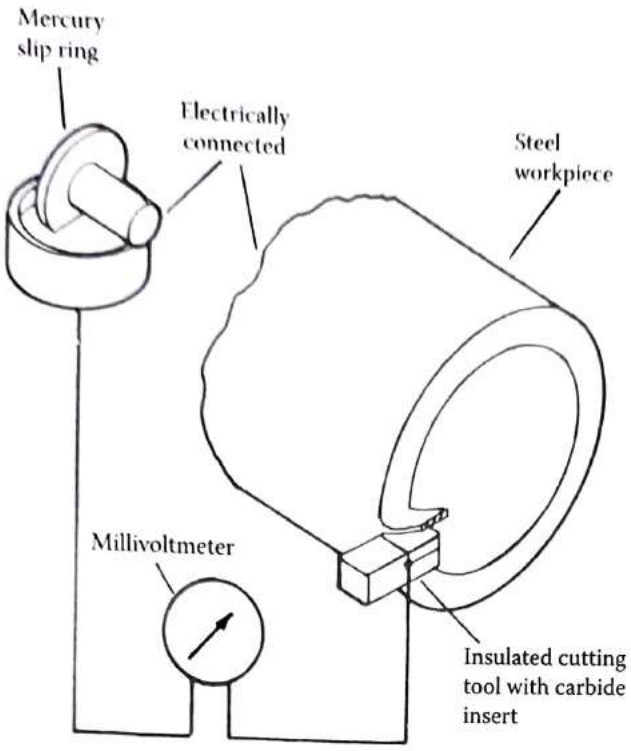

Fig. 18.4 Work-tool thermocouple circuit

There are a number of sources of error in using the work-tool thermocouple. In particular, the tool and work materials are not ideal elements for a thermocouple. Consequently, the emf tends to be low and the emf/temperature calibration nonlinear. The work-tool thermocouple must be calibrated against a standard thermocouple. Each tool and workpiece material combination must be calibrated separately. In addition, it is unlikely that the emf determined with a stationary tool, used for calibration, is the same as that obtained for an equivalent temperature during cutting when the work material is being severely strained.

B. DIRECT THERMOCOUPLE MEASUREMENTS

Direct thermocouple measurements can be made during cutting. In these experiments the rig was first run without cutting, and the reading on the milli-voltmeter resulting from the rubbing action of the constantan wire on the workpiece was noted.

This reading was subsequently subtracted from the readings taken while cutting was in progress. With this method, the temperatures at selected points around the end face of the tubular workpiece were measured and then used to calculate the proportion of the shear-zone heat conducted into the workpiece. Direct measurement of temperatures can be made by making a hole in the tool close to the cutting edge and inserting a thermocouple to measure the temperature at a particular position. This can then be repeated with holes in various positions to give an estimate of the temperature

distributions. Significant errors may occur where the temperature gradients are steep, as the holes for the thermocouples may cove r a considerable range of temperature. In addition, the presence of the holes may distort the heat flow and temperature fields in the tool.

C. RADATION METHODS

When the tool-workpiece area can be observed directly, cameras and film sensitive to infrared radiation can be used to deter mine temperature distributions. The result shown in Figure 18.5 was obtained from an infrared photograph of the cutting operation. In the technique used to produce this result a furnace of known temperature distribution was photographed simultaneously with the cutting operation using an infrared-sensitive plate, enabling the optical density of the plate to be calibrated against temperature.

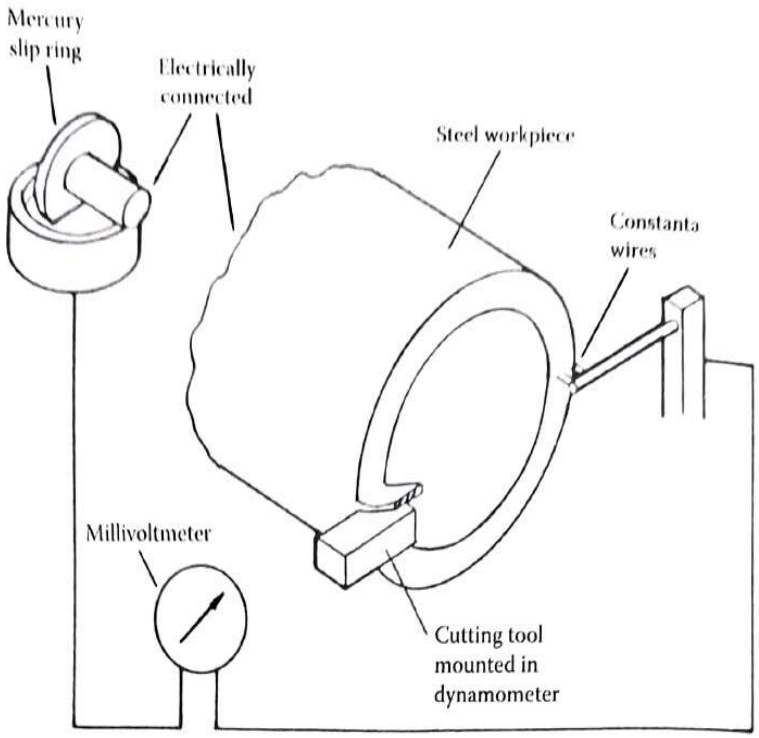

Fig.18.5 Arrangement for measurement of workpiece temperature s using the thermocouple technique.

For the result shown in Figure 18.2 the workpiece was preheated because of the relatively low sensitivity of the infrared photographic plates available at that time. Improvements in infrared-sensitive films and development of thermal imaging video cameras now make it possible to determine temperature distributions for workpieces at room temperature. Modern miniature electronic photo detectors arranged in a focal plane array system enable temperature distributions to be determined with resolutions as low as 5 µm.

D. HARDNES S AND MICROSTRUCTURE CHANGES IN STEEL TOOLS

The room-temperature hardness of hardened steel decreases after reheating, and the loss of hardness is related to the temperature and time of heating. The hardness decreases in the result of changes in the microstructure or the steel. These structural changes can be observed using optical and electron microscopes. These changes provide an effective means of determining temperature distributions in the tool during cutting. Microhardness measurements on tools after cutting can be used to determine constant-temperature contours in the tool, but the technique is time-consuming and requires very accurate hardness measurements.

The structural changes in the material take place gradually, but it has been observed that for some high-speed steels distinct modifications occur at approximately 50°C intervals between 600 and 900°C. This permits temperature measurements with an accuracy of ±25°C within the heat-affected region. Metallographic examination of the tool after cutting makes it possible for temperature distributions in the tool to be determined, but requires experienced interpretation of the observed structural changes. This method has been used to study temperature distributions in high-speed steel lathe tools and drills. The main limitation of this method of temperature estimation is that it can be used only within the range of cutting conditions suitable for high-speed steel and when relatively high temperatures are generated.

L 22.1 Factor Affecting the Temperature

Effect of Work Material

- Higher tensile strength of the material, greater the force is developed in the chip formation. Hence, more energy will be required for chip deformation and consequently more the heat generated followed by a higher cutting temperature.

- The higher the thermal conductivity of the work material, more heat is dissipated from the source into the chip formed and lower will be the temperature on the tool side.

- When machining harder materials, the area of contact of the chip with the tool surface is smaller. Thus, the intensity of pressure is higher over a smaller area of contact and the area for passage of heat into the tool is also smaller. This raise the temperature on the tool surface over a smaller area with greater concentration.

Effect of Cutting Variables

- Pm = Fc . Vc

  From above equation, that more heat will be generated with an increase in cutting speed.

- Cutting force increases with an increase of the feed. Consequently, the amount of heat involved will also increases.

- Work done increases with an increase in the depth, the amount of heat generated will also increases.

$$T = K. Vc^{z} . F^{x} . a^{y}$$

K = Constant characterizing the cutting condition

Vc = Cutting speed

f = Feed

a = Depth of cut

Effect of Tool Geometry

- **Rake Angle**
  - Reduction in rake angle increases the deformation and work done in chip formation leading to increase heat generation.
  - Chip contact area with tool face which improves heat removal into the tool thereby reducing the temperature at its contact surface.
  - A negative rake angle causes greater deformation than a positive angle leading to more heat generation.

- **Approach Angle**
  - Larger the approach angles the higher will be the cutting temperature.

- **Nose Radius**
  - The larger the nose radius the greater the deformation and tangential cutting force. More heat will be generated.

- **Cutting Fluid**
  - Suitable cutting fluid reduces the heat in the matter cutting by reducing the friction.
  - it's also absorbed the heat and carries it away, thereby lowering the temperature.